

DOI: <http://dx.doi.org/10.21123/bsj.2022.19.3.0704>

Syntheses, Structures and Biological Activity of Some Schiff Base Metal Complexes

Hassan M. A. Al-Redha¹

Safaa H. Ali^{2*}

Saad S. Mohammed³

¹Education Directory of Thi-Qar, Department of Education, Al-Shatrah, Thi-Qar, Iraq

²Department of Microbiology, College of Veterinary Medicine, University of Thi-Qar, Al-Shatrah, Thi-Qar, Iraq

³Department of Chemistry, College of Science, University of Thi-Qar, Al-Nasriyah, Thi-Qar, Iraq

*Corresponding author: safaa.ali@utq.edu.iq, hm942199@gmail.com, saad.sh-chem@sci.utq.edu.iq

*ORCID ID: <https://orcid.org/0000-0003-4924-7453>

Received 7/2/2021, Accepted 27/5/2021, Published Online First 20/11/2021, Published 1/6/2022



This work is licensed under a [Creative Commons Attribution 4.0 International License](https://creativecommons.org/licenses/by/4.0/).

Abstract:

Four new binuclear Schiff base metal complexes $[(MCl_2)_2L]$ $\{M = Fe\ 1, Co\ 2, Cu\ 3, Sn\ 4, L = N, N'-1,4\text{-Phenylenebis (methanylylidene) bis (ethane-1,2-diamine)}\}$ have been synthesized using direct reaction between proligand (L) and the corresponding metal chloride ($FeCl_2$, $CoCl_2$, $CuCl_2$ and $SnCl_2$). The structures of the complexes have been conclusively determined by a set of spectroscopic techniques (FT-IR, $^1H\text{-NMR}$, and mass spectra). Finally, the biological properties of the complexes have been investigated with a comparative approach against different species of bacteria (*E. coli* G-, *Pseudomonas* G-, *Bacillus* G+, *Staphylococcus* G+, and *Streptococcus* G+).

Keywords: Antibiotic, Metal complexes, Schiff base, Synthesis.

Introduction:

Over decades Schiff base continue attracts antibiotic designer's attention because of distinctive chelating features¹. Antibacterial activity of such ligand containing donor atoms can be enhanced significantly by coordination to a metal ion^{2, 3, 4}. Moreover, some natural molecules such as chlorophyll, hemoglobin, carbonic anhydrase, vitamin B12, xanthine oxides, and hemocyanin clearly indicate the important linkage between organic ligand and metal elements⁵. Scientists have been employed Schiff base in a wide range of medical applications such as antibacterial^{6, 7}, antifungal⁸, antitumor⁹, antiviral¹⁰, anti-HIV¹¹, herbicidal¹², and anti-influenza virus¹³.

In light of these medical facts, we present herein the synthesis, spectroscopic characterization and biological activity of a series of Schiff base metal complexes 1-4. Chemical analysis evidence allows proposing a binuclear aggregation mode for these M^{II} complexes of tetradentate Schiff-bases. The main objective of the present work was to find the antibacterial activity of these Schiff base metal complexes toward six different pathogens (*E. coli*

G-, *Pseudomonas* G-, *Bacillus* G+, *Staphylococcus* G+, and *Streptococcus* G+).

Material and Methods:

Chemical Materials

Terephthalaldehyde, 1,2-ethane-diamine, and metals chloride were purchased from commercial source Sigma-Aldrich and used as received. FT-IR spectra were recorded on a Bruker spectrometer. $^1H\text{-NMR}$ spectra were obtained using a Varian 400 NMR spectrometer in DMSO- d_6 , for all compounds using TMS as an internal standard. Mass analyses were performed on an Agilent Technology (HP) 5973 Network Mass Selective Detector. NMR and Mass spectra were collected at Department of Chemistry, Tehran University, Iran.

Ligands Synthesis

L (ligand) has been prepared as per literature procedure¹⁴ by refluxing terephthalaldehyde (0.13 g, 1 mmol) and (1,2-ethane-diamine) (0.12 g, 2 mmol) in methanol (Eqn. 1). After 4 h of continuous stirring, the reaction was cooled to 25 °C, filtered and dried in a desiccator over anhydrous $CaCl_2$. Orange powder of the Schiff

base (Yield = 0.20 g, 80%. mp. = 265-267 °C) was used for complexation without any further purification.

Schiff Base Metal Complexes Synthesis

Complexes 1-4 were synthesised by the direct addition of the Schiff base proligand (L) to metal chloride in 1:2 molar ratio (Eqn. 2). The mixture was dissolved in hot ethanol and the obtained solution was boiled for 4 h with reflux and continuous stirring led to form colored products¹⁵⁻¹⁷.

Physical and Spectral Data

[(FeCl₂)₂L] 1

An excellent yield of complex 1 (0.18 g, 85 %, m. p. 140-142 °C) was obtained from a typical metathesis reaction between FeCl₂ and L (equation 2). IR (KBr): $\tilde{\nu}$ = 3812 (w), 2578 (w), 2499 (w), 2293 (w), 2204 (w), 1929 (m), 1691 (w), 1608 (s), 1488 (s), 1439 (w), 1328 (s), 1211 (w), 1172 (s), 1098 (w), 1025 (s), 962 (s), 894 (s), 809 (s), 469 (s) Fig. (1). ¹H-NMR (400 MHz, DMSO, 25°C): δ = 8.51 (s, 4H, Ar), 3.90, (8H, CH₂), 2.50 (s, 2H, CH=N-). The molecular ion beam (M⁺) of the complex [(FeCl₂)₂L] was localized at m/z 386.00. This peak (calc. 315.01, found 322.00) attributed to NH₄Cl fragment. The large peak at 268.10 is related to the last ion after loses NH₄Cl CH₃CH₃.

[(CoCl₂)₂L] 2

Direct reaction between CoCl₂ and L in one pot {equation 2} leads to formed complex 2 in an excellent amount (0.19 g, 90 %, m. p. 251-253 °C). IR (KBr): $\tilde{\nu}$ = 3425 (w), 3026 (w), 2500 (w), 2368 (w), 2292 (w), 2053 (w), 1927 (m), 1602 (s), 1484 (s), 1436 (m), 1315 (s), 1168 (s), 1025 (s), 960 (s), 890 (s), 806 (s), 467 (s) Fig. (1). ¹H-NMR (400 MHz, DMSO, 25°C): δ = 8.49 (s, 4H, Ar), 3.26, (t, 8H, CH₂), 2.50 (s, 2H, CH=N-). The beam of molecular ion (M⁺) of the complex [(CoCl₂)₂L].6H₂O detected at 591.60 m/z. The Mass spectrum shows further two other peaks (calc. 567.94, found 577.60; calc. 549.93, found 551.60; calc. 477.89, found 480.50) (Fig. 10) corresponding to [(CoCl₂)₂L].5H₂O, [(CoCl₂)₂L].4H₂O and [(CoCl₂)₂L]⁺ respectively. Consequently, complex [(CoCl₂)₂L]⁺ lost Cl and NH₄ (calc. 440.93, found 437.40; calc. 425.92, found 423.40). Losing Cl and NH₄ showed the following peaks (calc. 390.95, found 393.30; calc. 375.94, found 381.40).

[CuCl₂)₂L] 3

Similarly, as described for complexes 1 and 2 complex [CuCl₂)₂L] (3) was synthesised in an excellent product (0.20 g, 95 %, m. p. 230-232 °C). IR (KBr): $\tilde{\nu}$ = 3302 (s), 3231 (s), 3122 (w), 2940 (m), 2883 (m), 2402 (w), 2342 (w), 2274 (w), 2194 (w), 2109 (w), 2050 (w), 1638 (m), 1571 (s), 1458 (m), 1361 (w), 1307 (w), 1270 (s), 1208 (w), 1128

(s), 1040 (s), 975 (m), 837 (w), 682 (s), 530 (s), 475 (m) Fig. (2). ¹H-NMR (400 MHz, DMSO, 25°C): δ = 3.33 (s, 4H, Ar), 2.50 (t, 8H, CH₂), 1.23 (br, 2H, CH=N-). The peak noticed at 577.60 m/z is related to [(CuCl₂)₂L].5H₂O⁺ the molecular ion. The following peaks (calc. 557.93, found 551.60; calc. 521.91 found 523.60; calc. 487.88, found 480.50) assigned to fragments [(CuCl₂)₂L].4H₂O, [(CuCl₂)₂L].2H₂O and [(CuCl₂)₂L]. Peaks at (calc. 472.87, found 468.40; calc. 385.93, found 393.40) attributed to (NH₄ and NH₄Cl) fragments. These peaks (Fig. 11) mentioned above prove the proposed structure for complex 2.

[(SnCl₂)₂L] 4

Complex 4 synthesized by following same route that described for complexes 1-3 in a moderate yield (0.16 g, 76 %, m. p. 269-271 °C). IR (KBr): $\tilde{\nu}$ = 3478 (w), 2580 (w), 2512 (w), 2388 (w), 2302 (w), 2053 (w), 1925 (w), 1693 (w), 1595 (s), 1487 (s), 1442 (w), 1327 (m), 1167 (m), 1029 (s), 965 (s), 901 (m), 813 (s), 777 (w), 606 (s), 477 (s) Fig. (3). ¹H-NMR (400 MHz, DMSO, 25°C): δ = 8.28 (s, 4H, Ar), 3.07 (t, 8H, CH₂), 2.50 (s, 2H, CH=N-). The peak at m/z 591.60 belongs to molecular ion of [(SnCl₂)₂L] (Fig. 12). Complex 4 further lost Cl and appeared at (calc. 560.86 found 563.50). Strong peak at (calc. 547.85 found 551.50) proving NH₄ fragment losing. The last ion further losing Cl and NH₄ were appeared at (calc. 510.88 found 509.50; calc. 495.87 found 495.40,) respectively. Differences in the isotopic abundance lead to a difference in overall mass thus, some fragments were shifted approximately two units than the calculated standard value.

In-vitro Antimicrobial Screening General Procedure

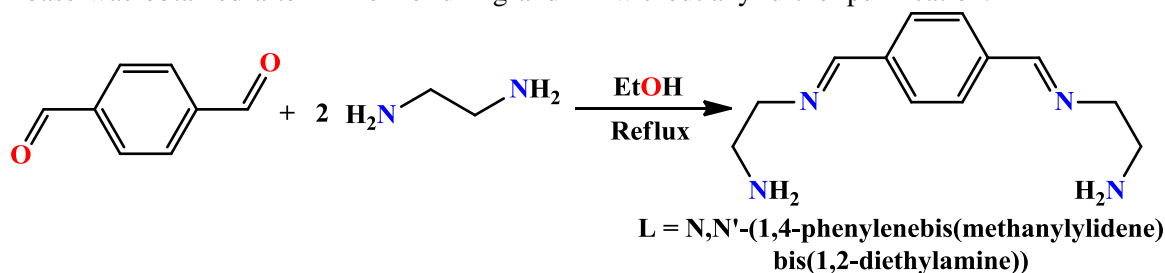
Pathogenic strains (*E. coli* G-, *Pseudomonas* G-, *Bacillus* G+, *Staphylococcus* G+, and *Streptococcus* G+) were used to screen biological activities of complexes [(FeCl₂)₂L] 1, [(CoCl₂)₂L] 2, [(CuCl₂)₂L] 3 and [(SnCl₂)₂L] 4. Disc diffusion method was employed in vitro. Microorganisms transfer to the nutrient agar under isolated atmosphere and using sterilised tools. Standard incubation method employed to complete diffusion. Dishes were kept at 25 °C for 1 h then placed in incubator at 37 °C for 24 h. Minimum inhibitory effect of the examined complexes was determined according to microwell dilution technique and Muller-Hinton broth used as a culture media. The tested compounds (1000 mg/ml) were heated to 50 °C for 30 min to increase solubility¹⁸.

Results and Discussion:

L proligand has been prepared according to previous reported procedure¹⁴ that involved condensation between terephthalaldehyde and 1,2-

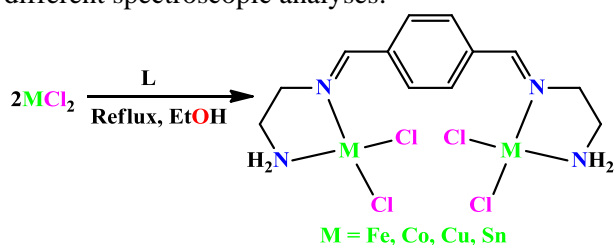
ethane-diamine (Eqn. 1). Orange powder of the Schiff base was obtained after 4 h of refluxing and

stirring the mixture and used for complexation without any further purification.



Equation 1

A similar synthesis strategy was adopted (Eqn. 2) to synthesise complexes 1-4. It is a simple one pot reaction involved 1:2 molar ratio between the proligand (L) and (FeCl_2 , CoCl_2 , CuCl_2 , SnCl_2) in ethanol that led to synthesise very stable complexes 1-4 toward air and moisture. DMSO is the only effective solvent toward these complexes. Solubility difficulties of complexes 1-4 blocked our path to obtain suitable single crystals for crystallography structures analysis in this study. Thus, complexes structures were confirmed through different spectroscopic analyses.



Equation 2

noticed between $1615\text{--}1620\text{ cm}^{-1}$ confirming ligand synthesis successfully¹⁸. The $\tilde{\nu}$ ($\text{C}=\text{N}$) moiety exhibit upward shift in 1697 (s) cm^{-1} after coordination to metal centre which is in agreement with the azomethine function that coordinated to metal ion of previous reported complexes¹⁹. The shift toward higher or lower frequencies is due to the interaction between the azomethine moiety and metal ions. Also, there are several factors that can affect the frequencies such as the metal ion nature and the coordination atoms. Moreover, medium bands that appear at $3535\text{--}2030\text{ cm}^{-1}$ of ligands may be assigned to $\tilde{\nu}$ NH group²⁰. Appearance of a strong bands at the range $695\text{--}270\text{ cm}^{-1}$ for all compounds is assignable to the $\tilde{\nu}$ ($\text{M}\text{--}\text{N}$) vibrations because of dimeric nuclear of the complex confirming the metal azomethine coordination^{21, 22}. The spectrum also gave an idea about the successful of ligand synthesis through the vanishing of the carbonyl ($\text{C}=\text{O}$) of aldehyde. The ($\text{C}\text{--}\text{H}$) aromatic vibrations is another evidence that is usually used to characterize Schiff bases depending on the bundles that appeared at the region ($3155\text{--}3030$).

FT-IR Spectra

FT-IR spectra of compounds 1-4 are in agreement with free ligand spectrum Figs. (1-4). Azomethine ($\text{C}=\text{N}$) group of the complexes 1-4 is

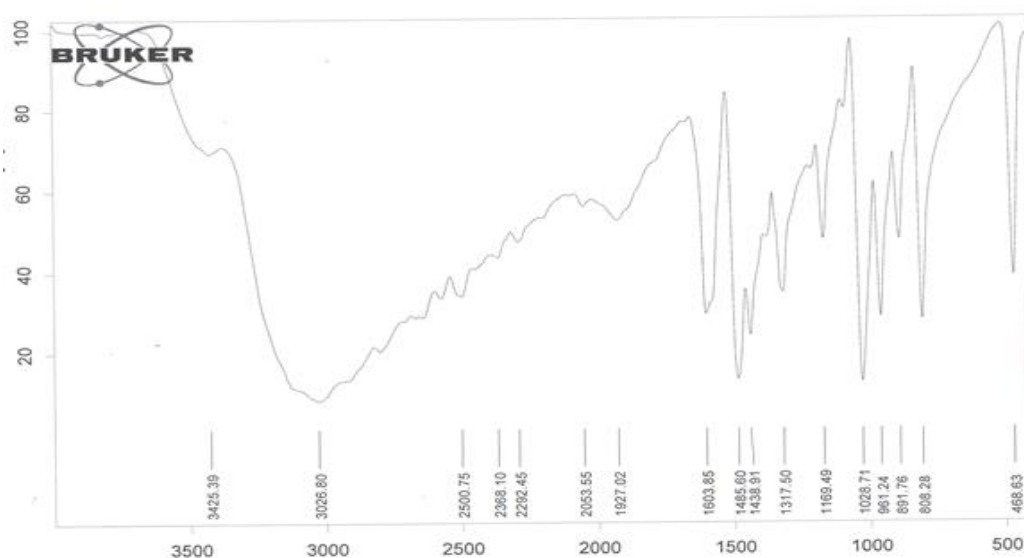


Figure 1. FT-IR spectrum of $[(\text{FeCl}_2)_2\text{L}]$ complex

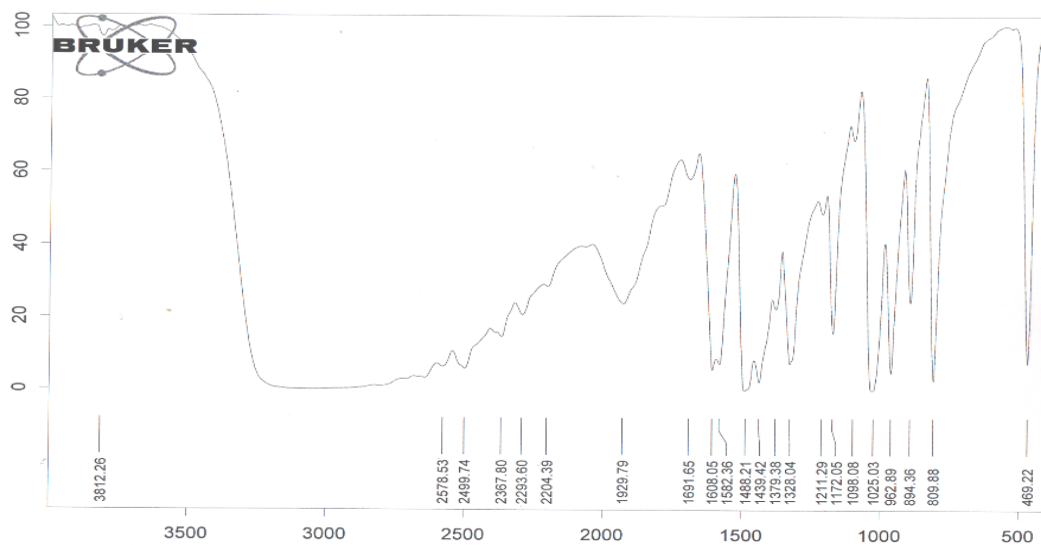


Figure 2. FT-IR spectrum of $[(CoCl_2)_2L]$ complex

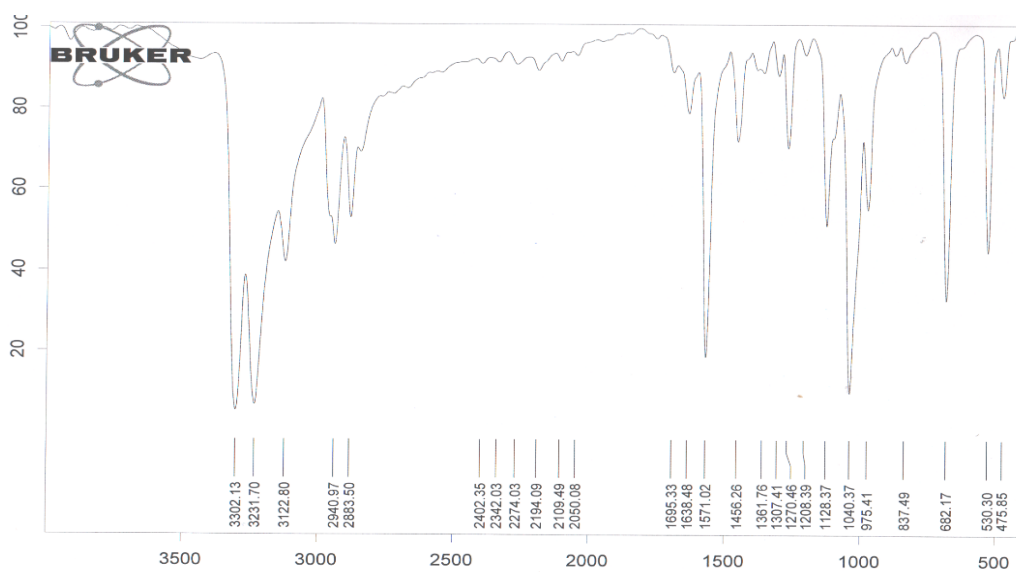


Figure 3. FT-IR spectrum of $[(CuCl_2)_2L]$ complex

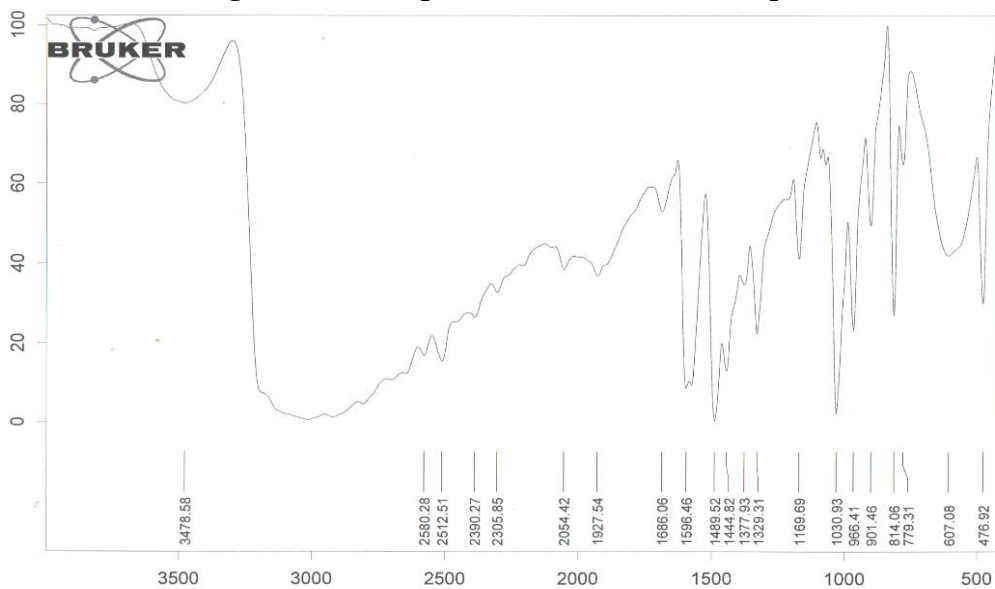


Figure 4. FT-IR spectrum of $[(SnCl_2)_2L]$ complex

¹H-NMR Spectra

The ¹H-NMR spectra of the complexes 1-4 were recorded in DMSO-d₆ at room temperature (Figs. 5-8). After complexation signals have shifted down or up field which can help to have better understand the behaviour of these complexes in solution. Because of the deshielding of protons, it is well known that the electron density reduces after bonding^{23, 24}. Moreover, the presence bimetallic species can increase the NMR spectra complexity due to the inequivalent in symmetry consequent of the dinuclear species.

Iron Schiff base complex [(FeCl₂)₂L] is further confirmed by NMR spectra. The ¹H-NMR spectrum given in Fig. (5) exhibited singlet beam in the aromatic region (8.51 ppm) assigned to the phenyl aromatic protons and the integrations calculation of those protons found to the correspond compound. The spectrum also shows one triplet bands notice at (3.90 ppm) to the methylene groups. Chemical integrations show the singlet that appeared at (2.50. ppm) related to azomethine. Noticeable overlap in signals due to the paramagnetic of Iron and dinuclear species that formed in solution which lead to increasing the ¹H-NMR spectra complexity²⁵. Cobalt Schiff base complex [(CoCl₂)₂L] was studied using ¹H-NMR spectroscopy that confirm the formation of fully condensed Schiff base complex. The triplet signal appearing in (3.26 ppm) of the ¹H-NMR spectra of cobalt complex are attributed to the methylene groups. In addition, independent signal is observed at 8.49 ppm related to aromatic protons of the phenyl group. The azomethine (HC=N) is observed at 2.50 ppm for [(CoCl₂)₂L]. The bonding between the nitrogen atom of azomethine and metal centre is proved by the downfield chemical shift observations. The aromatic signal is downfield shifted in the spectra of [(CuCl₂)₂L] complex due to the paramagnetic. Methylene group shows one signal at 2.50 ppm. Azomethine protons are affected and shifted down field in comparison between NMR spectra of complex with free ligand. The ¹H-NMR spectra of [(SnCl₂)₂L] complex exhibit a peak at 8.28 ppm, which is due to aromatic protons. The sharp singlet at 5.7 ppm and 6.047 ppm respectively assigned to for the (CH=N-) proton which clearly prove the magnetic effect that leads to up field shift in such protons²⁶. The azomethine signal is noticed at 2.50 ppm for [(SnCl₂)₂L]. The chemical shift belongs to the NH₂ protons in the proligand was not observed in any of the complexes 1-4. It is well known that such NH₂ protons did not detect so these peaks disappeared from spectrum.

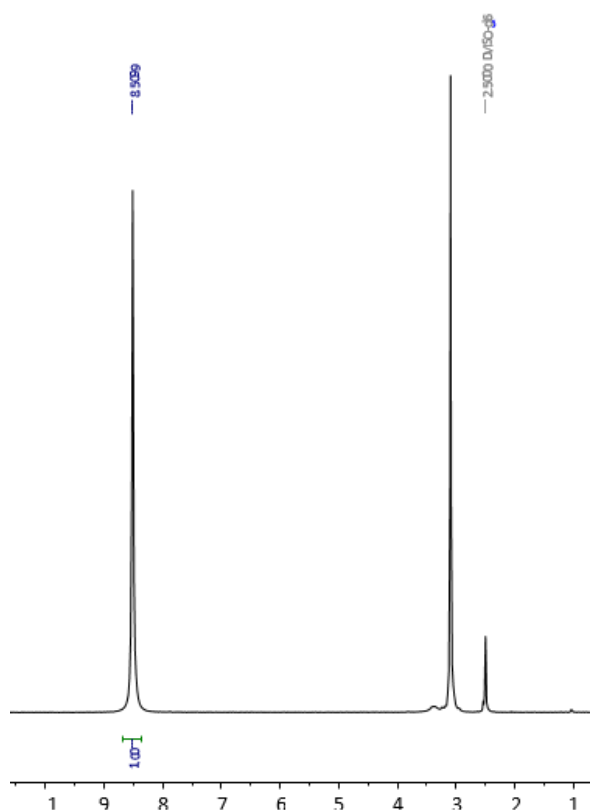


Figure 5. ¹H-NMR spectrum of [(FeCl₂)₂L]

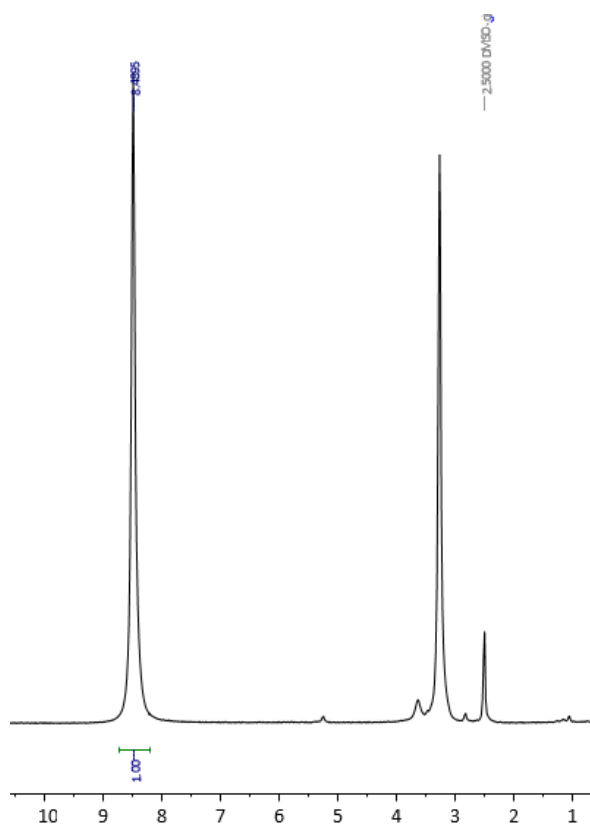


Figure 6. ¹H-NMR spectrum of [(CoCl₂)₂L]

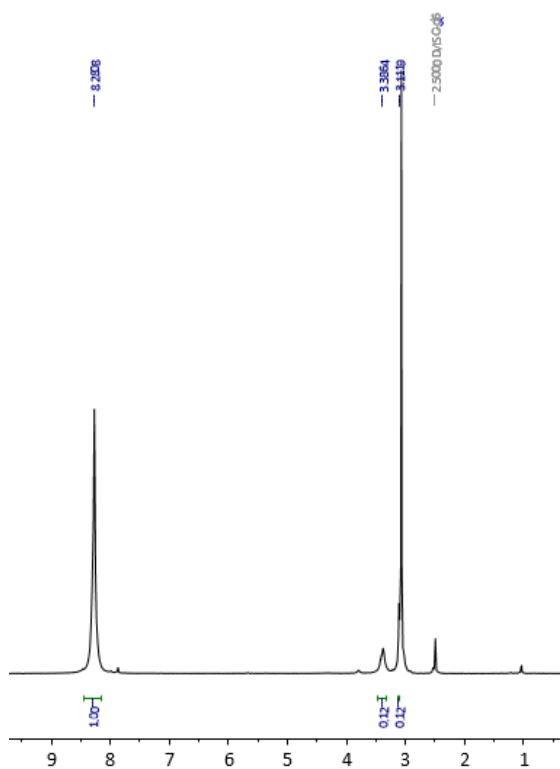


Figure 7. ¹H-MNR spectrum of [(CuCl₂)₂L]

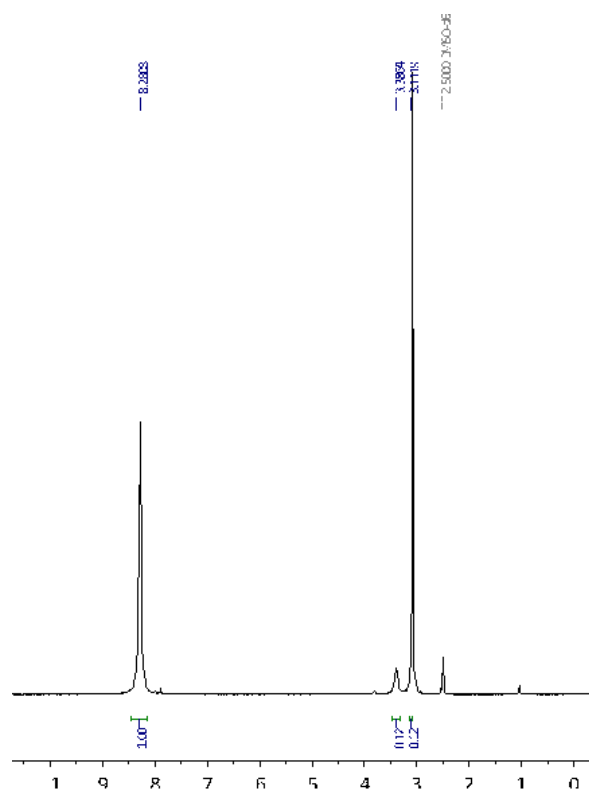


Figure 8. ¹H-MNR spectrum of [(SnCl₂)₂L]

Mass Spectra

Seventy V cone voltage are employed to complexes 1, 2, 3 and 4 to record mass spectra. Such voltage can minimise dissociation on ligand axial. Some peaks belong to a range of fragments that exhibited different values more or less than the calculated values. This behaviour is commonly known in mass spectra analysis due to the differences in isotopic abundance that occurred naturally for chemical elements. While, the voltage amount and the size of the substitution groups relatively can affect peak intensity.

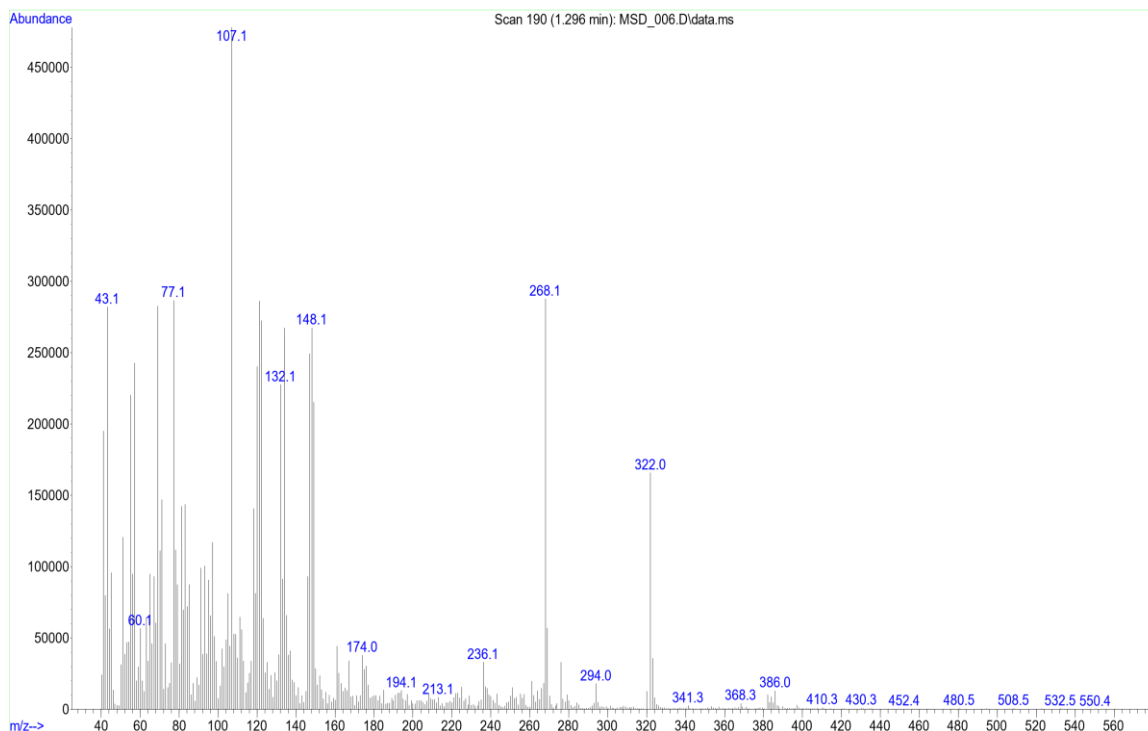


Figure 9. Mass spectrum of $[(FeCl_2)_2L]$ complex

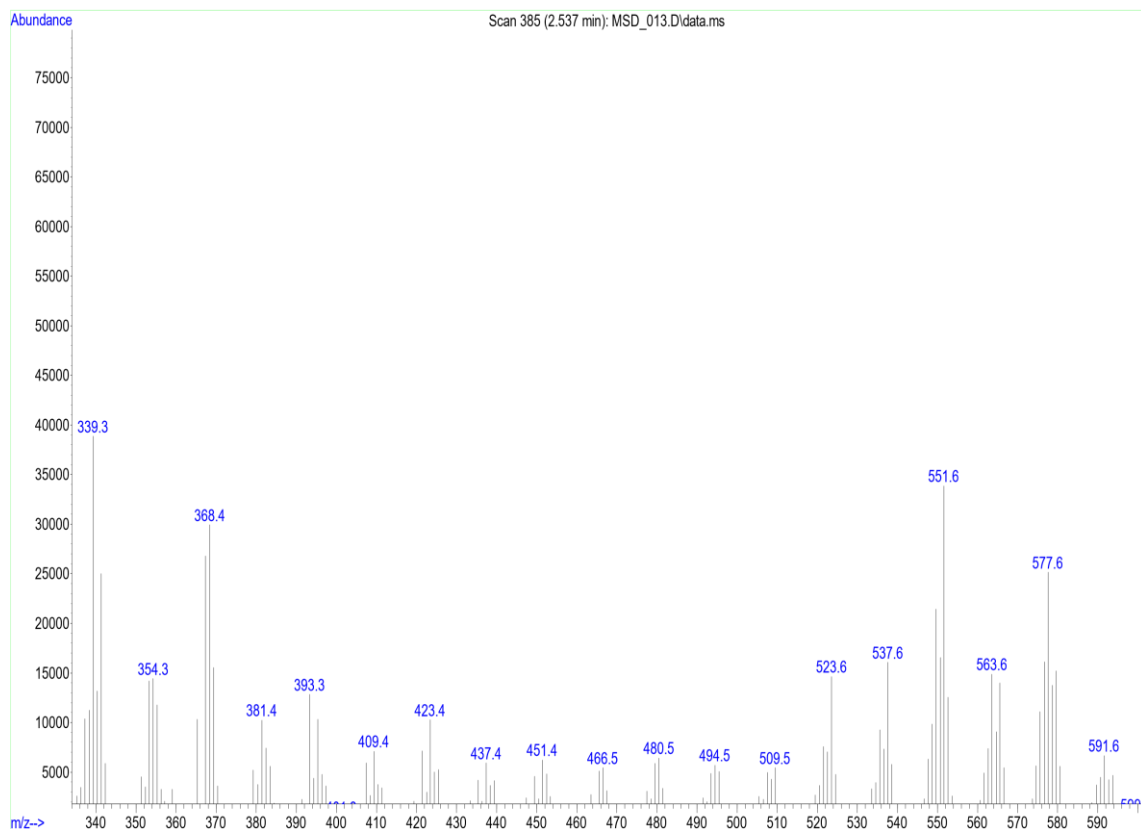


Figure 10. Mass spectrum of $[(CoCl_2)_2L]$ complex.

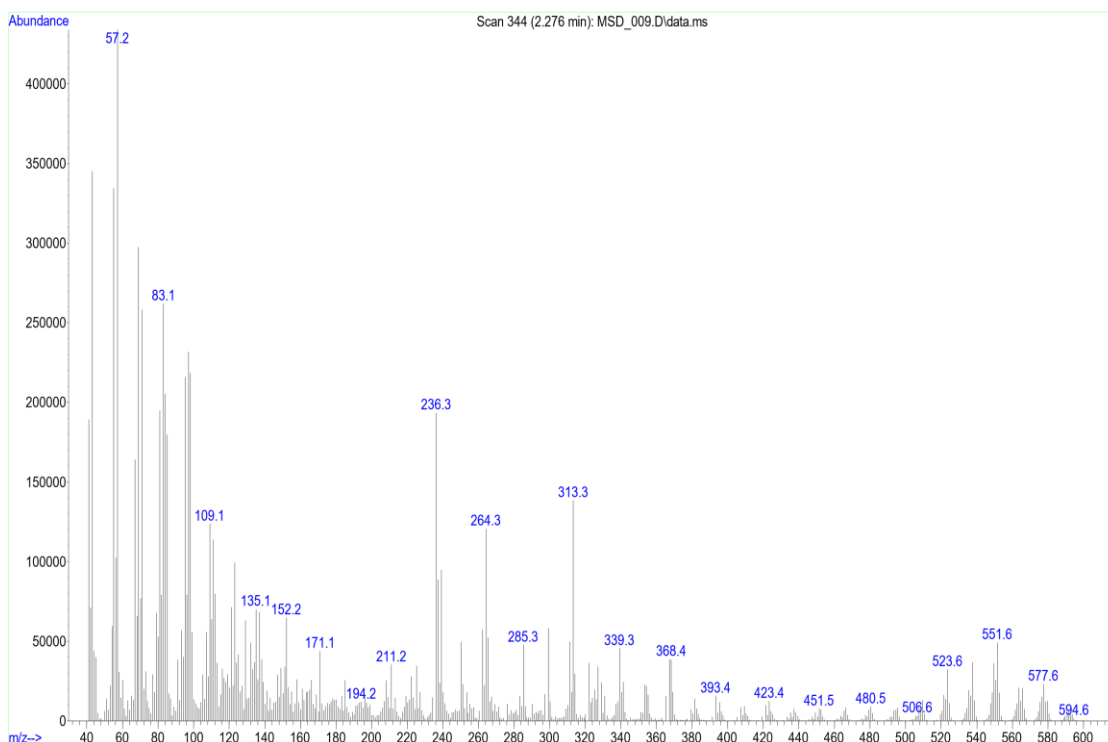


Figure 11. Mass spectrum of $[(\text{CuCl}_2)_2\text{L}]$ complex

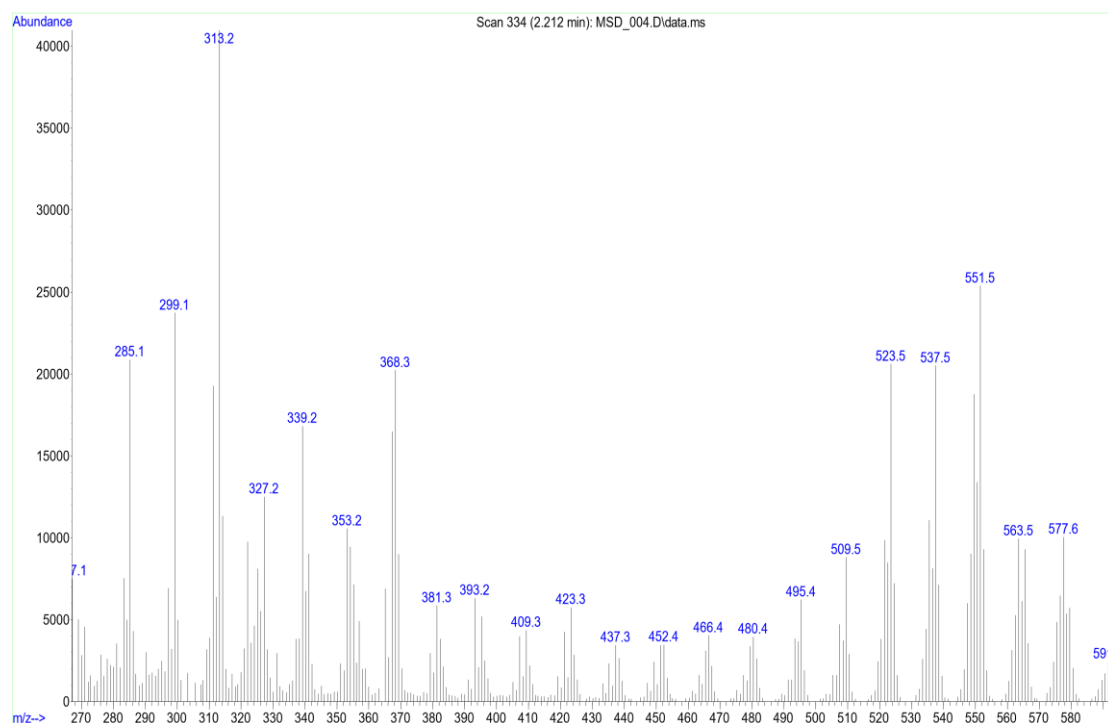


Figure 12. Mass spectrum of $[(\text{SnCl}_2)_2\text{L}]$ complex.

Biological Activity

The collected antibacterial results are presented in Table 1 according to the minimum inhibitory concentration and the inhibition zone. Anti-bacterial behavior of complexes 1, 2, 3, and 4 were screened in vitro toward a set of pathogens according to standards guidelines¹⁸ using disc

diffusion method and broth culture method. The minimum effective concentrations of compounds were also investigated. Complexes at low dose showed good to excellent inhibition toward tested bacteria (*E. coli* G-, *Pseudomonas* G-, *Bacillus* G+, *Staphylococcus* G+, and *Streptococcus* G+).

Table 1. The effects of chemical compounds (inhibition zone) on Gr- bacteria and Gr+ bacteria

*number = the number of compound appears on disc.

Chemical compounds	Isolates				
	<i>E. coli</i>	<i>Pseudomonas</i>	<i>Bacillus</i>	<i>Staphylococcus</i>	<i>Streptococcus</i>
[(FeCl ₂) ₂ L] (1) *5	3 mm	0 mm	0 mm	4 mm	0 mm
[(CoCl ₂) ₂ L] (2) *2	31mm	34 mm	38 mm	37 mm	35 mm
[(CuCl ₂) ₂ L] (3) *3	35 mm	32 mm	30 mm	30 mm	33 mm
[(SnCl ₂) ₂ L] (4) *4	20 mm	30 mm	19 mm	27 mm	31 mm

[(FeCl₂)₂L] metal complex showed a small inhibition zone (3 mm) on *E. coli* G- growth and did not exhibit any destruction action against *Pseudomonas* G- (0 mm). While in comparison with complex 1 complexes 2-4 exhibited significant inhibition activity toward *E. coli* G- and *Pseudomonas* G- Table 1 (Fig. 13 and 14). Complex 1 also was found to have very limited destruction activity (4 mm) on *Staphylococcus* G+ and appear to have no growth inhibition activity on *Bacillus* G+ and *Streptococcus* G+ with MIC values (0 mm) Table 1 (Fig. 15, 16 and 17). Complexes [(CoCl₂)₂L] and [(CuCl₂)₂L] exhibit approximately a similar appreciable antibacterial activity against all screened pathogens with minimum inhibition zones ranged (30-38 mm, Figs. 13, 14, 15, 16, 17, Table 1). While complex [(SnCl₂)₂L] was found to be less active than [(CoCl₂)₂L] and [(CuCl₂)₂L] but more active than [(FeCl₂)₂L] against examined gram negative and gram positive bacteria. It showed moderate to good antibacterial activity ranged (19-31 mm, Figs. 13, 14, 15, 16, 17, Table 1). As seen in (Figs. 13, 14, 15, 16, 17, Table 1), tested compounds 2-4 clearly showed promising inhibition activity against the selected gram-negative and gram-positive pathogens. Collected biological data in this study is compatible with previously published studies of Schiff base metal compounds²⁷⁻³⁰. Complex [(FeCl₂)₂L] did not show any destruction activity toward *Pseudomonas*, *Bacillus*, and *Streptococcus*. However, it showed very limited inhibition activity toward *E. coli* and *Staphylococcus*.



Figure 13. Shows inhibition zones of *E. coli* G- by the effect of (1, 2, 3 and 4) was (13, 15, 20 and 13 mm).



Figure 14. Shows inhibition zones of *Pseudomonas* G- by the effects of (1, 2, 3 and 4) was (4, 28, 45 and 48 mm) respectively.

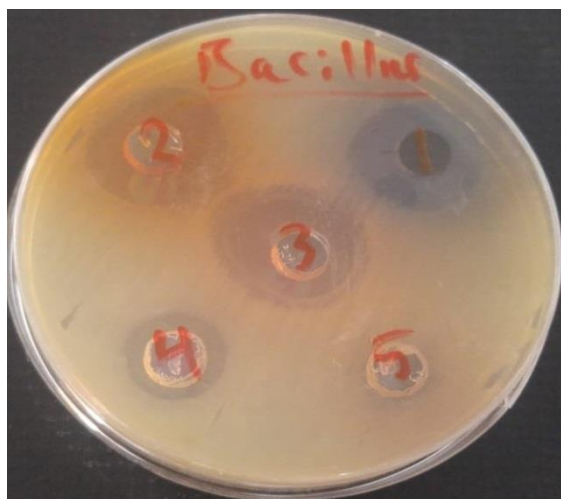


Figure 15. Shows inhibition zone of *Bacillus* G+ by the effects of (1, 2, 3 and 4) were (0, 25, 30 and 15 mm) respectively.

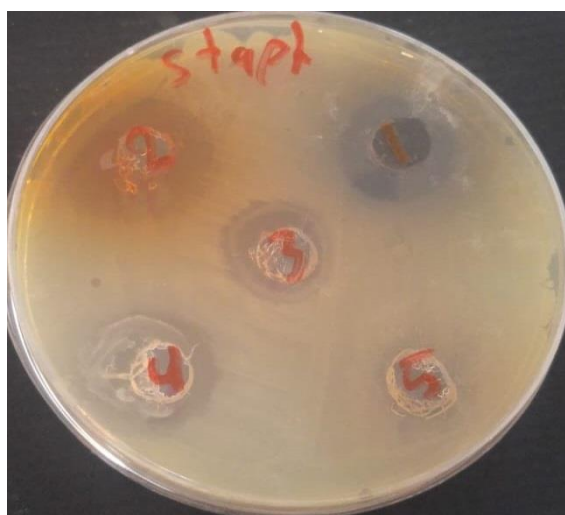


Figure 16. Shows inhibition zone of *Staphylococcus* G+ by the effects of (1, 2 and 3) was (0, 0, 0 and 0 mm) respectively.



Figure 17. Shows inhibition zones of *Streptococcus* G+ by the effect of (1, 2, 3 and 4) was (22, 0, 0 and 42mm).

Conclusions:

Schiff base metal complexes $[(MCl_2)_2L]$ were synthesized as mentioned before²¹⁻²³. Complexes exhibit an excellent stability toward air and mixture. These complexes 1-4 were synthesized and characterized by different techniques. The melting points, Mass spectra, IR, and ¹H-NMR, confirmed the formation of the binuclear complexes. A distorted square planar geometry was proposed for the metal centers of complexes (1-4) based on structure analysis. Complexes revealed promising antibacterial activities toward different pathogenic strains of bacteria (*E. coli* G-, *Pseudomonas* G-, *Bacillus* G+, *Staphylococcus* G+, and *Streptococcus* G+).

Acknowledgments

Authors gratefully acknowledge technical support from University of Thi-Qar.

Authors' declaration:

- Conflicts of Interest: None.
- We hereby confirm that all the Figures and Tables in the manuscript are mine ours. Besides, the Figures and images, which are not mine ours, have been given the permission for re-publication attached with the manuscript.
- Ethical Clearance: The project was approved by the local ethical committee in University of Thi-Qar.

Authors' contributions statement

S.H. Ali, H.M.A. Al-Redha and S.S. Mohammed are contributed to the design and implementation of the research, to the analysis of the results and to the writing of the manuscript

References:

1. Radha VP, Kirubavathy SJ, Chitra S. Synthesis, characterization and biological investigations of novel Schiff base ligands containing imidazoline moiety and their Co (II) and Cu (II) complexes, *J. Mol. Struct.* 2018; 1165, 246-258. <https://doi.org/10.1016/j.molstruc.2018.03.109>
2. Xu X, Ma S, Wu J, Yang J, Wang B, Wang S, Zhu J. High-performance, command degradable, antibacterial Schiff base epoxy thermosets: synthesis and properties. *J. Mater. Chem. A.* 2019; 7(25): 15420-15431. <https://doi.org/10.1039/C9TA05293C>
3. Khalid KL. Some metal ions complexes derived from schiff base ligand with anthranillic acid: preparation, spectroscopic and biological studies. *Baghdad Sci. J.* 2020. 17 (1): 0099. <https://doi.org/10.21123/bsj.2020.17.1.0099>
4. Chohan ZH, Arif M, Sarfraz M. Metal based antibacterial and antifungal amino acid derived Schiff bases: their synthesis, characterization and in vitro

- biological activity, *Appl. Organomet. Chem.* 2007; 21(4): 294-302. <https://doi.org/10.1002/aoc.1200>
5. Rana BS, Jain SL, Singh B, Bhaumik A, Sain B, Sinha AK. Click on silica: systematic immobilization of Co (II) Schiff bases to the mesoporous silica via click reaction and their catalytic activity for aerobic oxidation of alcohols. *Dalton Trans.* 2010; 39(33): 7760-7767. <https://doi.org/10.1039/C0DT00208A>
6. Hwang S, Ryu JY, Jung SH, Park HR, Lee J. Cobalt complexes containing salen-type pyridoxal ligand and DMSO for cycloaddition of carbon dioxide to propylene oxide. *Polyhedron*, (2020); 178, 114353. <https://doi.org/10.1016/j.poly.2020.114353>
7. Panneerselvam P, Rather BA, Reddy DRS, Kumar NR. Synthesis and anti-microbial screening of some Schiff bases of 3-amino-6, 8-dibromo-2-phenylquinazolin-4 (3H)-ones, *Eur. J. Med. Chem.* 2009; 44(5): 2328-2333. <https://doi.org/10.1016/j.ejmech.2008.04.010>
8. Rai BK, Kumar A. Synthesis, characterization and biocidal activity of some Schiff base and its metal complexes of Co (II), Cu (II) and Ni (II), *Orient. J. Chem.* 2013; 29(3): 1187-1191. <http://dx.doi.org/10.13005/ojc/290349>
9. Ali SH, Abed HM, Abdulhussein HS. Antibiotic activity of new species of Schiff base metal complexes. *Periódico Tchê Química.* 2020; 17 (35): 837-860. <http://deboni.he.com.br/Periodico35.pdf>
10. Illán-Cabeza NA, Hueso-Urena F, Moreno-Carretero MN, Martínez-Martos JM, Ramírez-Expósito MJ. Synthesis, characterization and antiproliferative activity of metal complexes with the Schiff base derived from the condensation 1: 2 of 2, 6-diformyl-4-methylphenol and 5, 6-diamino-1, 3-dimethyluracil. *J. Inorgan. Biochem.* 2008; 102 (4): 647-655. <https://doi.org/10.1016/j.jinorgbio.2007.10.008>
11. Kumar KS, Ganguly S, Veerasamy R, De Clercq E. Synthesis, antiviral activity and cytotoxicity evaluation of Schiff bases of some 2-phenyl quinazoline-4 (3) H-ones, *Eur. J. Med. Chem.* 2010; 45(11): 5474-5479. <https://doi.org/10.1016/j.ejmech.2010.07.058>
12. Roy S, Dutta T, Drew MG, Chattopadhyay S. Phenoxazinone synthase mimicking activity of a dinuclear copper (II) complex with a half salen type Schiff base ligand. *Polyhedron*, 2020; 178, 114311. <https://doi.org/10.1016/j.poly.2019.114311>
13. Illán-Cabeza NA, García-García AR, Martínez-Martos JM, Ramírez-Expósito MJ, Moreno-Carretero M N. Antiproliferative effects of palladium (II) complexes of 5-nitrosopyrimidines and interactions with the proteolytic regulatory enzymes of the renin-angiotensin system in tumoral brain cells. *J. Inorgan. Biochem.* 2013; 126, 118-127. <https://doi.org/10.1016/j.jinorgbio.2013.06.005>
14. Zhao X, Li C, Zeng S, Hu W. Discovery of highly potent agents against influenza A virus, *Eur. J. Med. Chem.* 2011; 46(1): 52-57. <https://doi.org/10.1016/j.ejmech.2010.10.010>
15. Azam M, Al-Resayes SI, Trzesowska-Kruszynska A, Kruszynski R, Adil SF, Lokanath NK. Pyridine solvated dioxouranium complex with salen ligand: Synthesis, characterization and luminescence properties." *J. Saudi Chem. Soc.* 2019; 23(5): 636-641. <https://doi.org/10.1016/j.jscs.2019.01.006>
16. Mishra M, Tiwari K, Mourya P, Singh MM, Singh P. Synthesis, characterization and corrosion inhibition property of nickel (II) and copper (II) complexes with some acylhydrazine Schiff bases, *Polyhedron.* 2015; 89, 29-38. <https://doi.org/10.1016/j.poly.2015.01.003>
17. Salehi M, Ghasemi F, Kubicki M, Asadi A, Behzad M, Ghasemi MH, Gholizadeh A. Synthesis, characterization, structural study and antibacterial activity of the Schiff bases derived from sulfanilamides and related copper (II) complexes, *Inorgan. Chim. Acta.* 2016; 453, 238-246. <https://doi.org/10.1016/j.ica.2016.07.028>
18. Nagesh GY, Mruthyunjayaswamy BHM. Synthesis, characterization and biological relevance of some metal (II) complexes with oxygen, nitrogen and oxygen (ONO) donor Schiff base ligand derived from thiazole and 2-hydroxy-1-naphthaldehyde, *J. Mol. Struct.* 2015; 1085, 198-206. <https://doi.org/10.1016/j.molstruc.2014.12.058>
19. Mucbe S, Levacheva I, Samsonova O, Biernasiuk A, Malm A, Lonsdale R, Popiołek Ł, Bakowsky U, Hołynska M. Synthesis, structure and stability of a chiral imine-based Schiff-based ligand derived from L-glutamic acid and its [Cu₄] complex. *J. Mol. Struct.* 2017; 1127, 231-236. <https://doi.org/10.1016/j.molstruc.2016.07.100>
20. Das M, Chatterjee S, Harms K, Mondal TK, Chattopadhyay S. Formation of bis (μ-tetrazolato) dinickel (II) complexes with N, N, O-donor Schiff bases via in situ 1, 3-dipolar cyclo-additions: isolation of a novel bi-cyclic trinuclear nickel (II)-sodium (I)-nickel (II) complex, *Dalton Trans.* 2014; 43(7): 2936-2947. <https://doi.org/10.1039/C3DT52796D>
21. Khan S, Jana S, Drew MGB, Bauzá A, Frontera A, Chattopadhyay S. A novel method for copper (II) mediated region-selective bromination of aromatic rings under mild conditions, *RSC advances.* 2016; 6(66): 61214-61220. <https://doi.org/10.1039/C6RA13215D>
22. Khan S, Masum AA, Islam MM, Drew MGB, Bauzá A, Frontera A, Chattopadhyay S. Observation of π-hole interactions in the solid state structures of three new copper (II) complexes with a tetradentate N4 donor Schiff base: Exploration of their cytotoxicity against MDA-MB 468 cells, *Polyhedron.* 2017; 123, 334-343. <https://doi.org/10.1016/j.poly.2016.11.012>
23. Bhattacharyya A, Sen S, Harms K, Chattopadhyay S. Formation of three photoluminescent zinc (II) complexes with Zn₂O₂ cores: Examples of bi-dentate bonding modes of potentially tri-and tetra-dentate Schiff bases, *Polyhedron.* 2015; 88, 156-163. <https://doi.org/10.1016/j.poly.2014.12.018>
24. Mahmoud WA, Hassan ZM. Synthesis and spectral analysis of some metal ions complexes with mixed ligands of Schiff base and 1, 10-phenanthroline. *Baghdad Sci. J.* 2017; 14 (1):0135. <https://doi.org/10.21123/bsj.2017.14.1.0135>

25. Nazir U, Akhter Z, Janjua NK, Asghar MA, Kanwal S, Butt TM, Shah FU. Biferrocenyl Schiff bases as efficient corrosion inhibitors for an aluminium alloy in HCl solution: a combined experimental and theoretical study. *RSC Advances*, 2020; 10(13): 7585-7599. <https://doi.org/10.1039/C9RA10692H>
26. Keypour H, Zebarjadian MH, Rezaeivala M, Chehreghani A, Amiri-Rudbari H, Bruno G. Synthesis, characterization, crystal structure and antibacterial studies of some new heptadentate manganese (II), cadmium (II) and zinc (II) macrocyclic Schiff base complexes with two 2-pyridylmethyl pendant arms, *J. Iranian Chem. Soc.* 2014; 11(1): 101-109. <https://doi.org/10.1007/s13738-013-0280-y>
27. Murugaiyan M, Mani SP, Sithique MA. Zinc (ii) centered biologically active novel N, N, O donor tridentate water-soluble hydrazide-based O-carboxymethyl chitosan Schiff base metal complexes: synthesis and characterisation. *New J. Chem.* 2019; 43(24), 9540-9554. <https://doi.org/10.1039/C9NJ00670B>
28. Gündüzalp AB, Özsen I, Alyar H, Alyar S, Özbek N. Active Schiff bases containing thiophene/furan ring and their copper (II) complexes: Synthesis, spectral, nonlinear optical and density functional studies, *J. Mol. Struct.* 2016; 1120, 259-266. <https://doi.org/10.1016/j.molstruc.2016.05.002>
29. Zuleta EC, Goenaga GA, Zawodzinski TA, Elder T, Bozell JJ. Deactivation of Co-Schiff base catalysts in the oxidation of para-substituted lignin models for the production of benzoquinones. *Catal. Sci. Technol.* 2020; 10(2): 403-413. <https://doi.org/10.1039/C9CY02040C>
30. Gündüzalp AB, Özbek N, Karacan N. Synthesis, characterization, and antibacterial activity of the ligands including thiophene/furan ring systems and their Cu (II), Zn (II) complexes, *Med. Chem. Res.* 2012; 21(11): 3435-3444. <https://doi.org/10.1007/s00044-011-9878-8>

تخليق وتشخيص ودراسة الفعالية البيولوجية لعدد من معقدات قواعد شف

سعد شهد محمد³

صفاء حسين علي²

حسن موازي عبد الرضا¹

¹ مديرية تربية ذي قار، الشطرة، العراق

² كلية الطب البيطري، جامعة ذي قار، الشطرة، العراق

³ كلية العلوم، جامعة ذي قار، الناصرية، العراق

الخلاصة:

اربع معقدات قاعدة شف ثنائية النواة جديدة $[(MCl_2)_2L]$ { (4) Sn، (3) Cu، (2) Co، Fe (1) = M } ليكاند = 1,4-ثنائي فنيولين (ميثان دابيين) ثنائي (اثنان ثنائي امين). حضرت بطريقة التفاعل المباشر بين اليكاند وعدد من هاليدات الفلزات. الصيغ التركيبية للمركبات اثبتت من خلال عدد من التقنيات الطيفية مكيف الاشعة تحت الحمراء وطيف الرنين النووي المغناطيسي وطيف الكتلة. حددت الفعالية الحيوية للمركبات تجاه عدد من العزلات البكتيرية السالبة والموجبة الغرام مثل العصية القولونية، الزوائف، العصيات، المكورات العنقودية، المسببات العنقودية.

الكلمات المفتاحية: مضادات بكتيرية، معقدات لاعضوية، شف بيز، تخليق